이학석사 학위논문

Effect of the Molecular Weight Distribution of the Hydrophobic Block on the Solution Self-Assembly of Block Copolymers having a Branched Hydrophilic Block with a Discrete Molecular Weight

분자량 분포가 없는 친수성 블록을 가진 블록 공중합체의 수용액 상 자기조립에 대한 소수성 블록의 분자량 분포의 영향

2019 년 8 월

서울대학교 대학원

화학부 고분자화학 전공

하 성 민

ABSTRACT

Effect of the Molecular Weight Distribution of the Hydrophobic Block on the Solution Self-Assembly of Block Copolymers having a Branched Hydrophilic Block with a Discrete Molecular Weight

Sungmin Ha

Polymer Chemistry in Department of Chemistry

The Graduate School

Seoul National University

The molecular weight distribution (MWD) of polymer blocks constituting block copolymers (BCPs) directly influences their self-assembly in the bulk and the resulting periodic nanostructures. However, the effect of the MWD of core-forming hydrophobic blocks on the structures of BCPs self-assembled in solution has rarely been studied in relation to the formation of highly ordered mesophases. Herein, we report the effects of core-forming hydrophobic block MWD on the formation of bicontinuous cubic mesophases of BCPs in solution. Specifically, a series of BCPs with tunable-MWD hydrophobic blocks is prepared by coupling a discrete ($Đ$ = 1.0)

branched poly(ethylene glycol) (bPEG) hydrophilic block with a hydrophobic polystyrene (PS) block with the desired MWD. The MWDs of PS blocks were adjusted by controlling the addition rate of the initiator for the atom-transfer radical polymerization of styrene, with the resulting $Đ$ values ranging from 1.08 to 1.72.

The solution self-assembly of the thus produced branched-linear BCPs (bPEG-PS) indicated that an increase of PS block $Đ$ value from 1.09 to 1.72 resulted in a gradual deterioration of the internal order of bPEG-PS polymer cubosomes from a cubic crystalline phase to a disordered cubic and sponge phase. It was concluded that the MWD of the core-forming hydrophobic block is the major parameter determining the internal structure disorder of polymer cubosomes. In addition, when the $Đ$ value of the core-forming hydrophobic PS block of bPEG-PS was increased at constant M_n, the dominant symmetry of self-assembled cubosomes changed from $Pn\bar{3}m$ to $Im\bar{3}m$.

Keywords : block copolymer, molecular weight distribution, dispersity, solution self-assembly, cubosome

Student Number : 2017-24686

Table of Contents

List of Figures, Schemes, and Tables

Figures

Schemes

Tables

I. INTRODUCTION

The effect of the molecular weight distribution (MWD) of block copolymers (BCPs) on their self-assembly in the bulk has been extensively studied in terms of morphology, size of segregated polymer domains, and order-disorder transition temperature of self-assembled nanostructures.[1–4] Lynd et al. found that an increase in $Đ$ of poly(DL-lactide) of poly(ethylene-*alt*-propylene)-*b*-poly(DL-lactide) at constant block ratio led to increased domain or lattice spacing of the self-assembled lamellar phase.[1,2,4] They also discovered morphological transitions favoring structures with increased curvature toward the poly(DL-lactide) presumably due to the reduced stretching energy of the disperse component.[1,4] The same group also demonstrated that increasing $Đ$ in the minority or majority component of poly(ethylene-*alt*-propylene)-*b*-poly(DL-lactide) or polystyrene-*b*-polyisoprene resulted in a decrease or an increase in the segregation strength at the order–disorder transition.[3,4]

In contrast, the influence of MWD on the solution self-assembly of amphiphilic BCPs has been underexplored. Terreau et al. showed that an increase of the MWD of the poly(acrylic acid) block, indicated by the magnitude of $Đ$, led to the self-assembly of polystyrene-*b*-poly(acrylic acid) to form smaller vesicles because of the segregation between chains with different lengths.[5] This result was theoretically supported by Jiang et al., who used two-dimensional real-space self-consistent-field theory (2D SCFT) to show that a larger MWD of amphiphilic diblock copolymers resulted in the formation of smaller vesicles or quasi-vesicles.[6] Terreau et al. also observed that increasing the $Đ$ of a block copolymer induces sphere-to-rod-to-vesicle morphological transitions under certain self-assembly conditions.[7] In contrast, Li et al. employed 2D SCFT to demonstrate that an increase of the $Đ$ of amphiphilic diblock copolymers leads to a vesicle-to-micelle transition.[8] Recently,

Meijer and co-workers demonstrated the effect of $Đ$ on assembly behavior both in the bulk and in solution by comparing discrete and disperse amphiphilic oligomers.[9] However, when investigating the effect of $Đ$ on self-assembly behavior, the aforementioned studies focus on relatively simple morphologies such as micelles, cylindrical micelles, vesicles, and 2D sheets.

Colloidal particles of inverse bicontinuous cubic mesophases (polymer cubosomes) are emerging nanostructures created by the direct self-assembly of BCPs in solution. Polymer cubosomes feature triply periodic minimal surfaces comprising bilayers of BCPs with cubic crystalline symmetry. The symmetry of the internal cubic lattices of polymer cubosomes is determined by the BCP block ratio, which, in turn, is defined by the molecular weight fraction of the hydrophilic block. For example, diblock copolymers comprising branched poly(ethylene glycol) (PEG) and PS blocks (bPEG-PS) self-assemble to form vesicles, lamellae, hexosomes, and cubosomes with internal Schwarz P ($Im\bar{3}m$ symmetry) or Schwarz D ($Pn\bar{3}m$ symmetry) surfaces depending on the block ratio of the branched-linear BCP.[10–15] Considering the narrow window of the BCP block ratio required to direct the self-assembly to form a specific lattice, the MWD of the BCP should be constrained to be as narrow as possible by adopting controlled radical polymerization methods to synthesize the hydrophobic PS block. In previous studies on the formation of polymer cubosomes via BCP self-assembly, the BCP $Đ$ value was less than 1.2.[10–16] However, the effects of the MWD of BCPs on their complex morphologies such as inverse bicontinuous cubic mesophases self-assembled in solution have not been studied yet.

Herein, we investigate the influence of $Đ$ on the solution self-assembly of a series of bPEG-PSs, by adjusting the $Đ$ of the hydrophobic PS block.[10,11] To eliminate the influence of the $Đ$ of the hydrophilic block, we adopted an iterative

coupling strategy to synthesize a discrete ($Đ$ = 1.0) PEG starting from commercially available tetraethylene glycol for building the branched PEG block.[17,18] Hydrophobic PS blocks with $Đ$ > 1.4 were synthesized by adopting a temporal regulation of initiation strategy, wherein the initiator addition rate was adjusted during atom-transfer radical polymerization (ATRP) instead of nitroxide-mediated or anionic polymerizations reported by Fors and co-workers.[19–22] The solution self-assembly of the resulting branched-linear BCPs (bPEG-PS) indicated that as the $Đ$ of the PS block increased from 1.09 to 1.72, the internal order of bPEG-PS cubosomes changed from a cubic crystalline phase to a disordered cubic and sponge phase.

II. RESULTS AND DISCUSSION

Synthesis of bPEG-PS with the desired hydrophobic block MWD.

We designed a BCP with a discrete ($Đ$ = 1.0) hydrophilic block so that the effect of the hydrophobic block MWD on BCP self-assembly could be investigated without obscuration by the hydrophilic block MWD. PEG with 12 ethylene oxy units was synthesized by iterative coupling of tetraethylene glycol (Figure 10).[17,18] The resulting α-tosyl-ω-trityl PEG (**1**) was tethered to a methyl benzoate core, which was followed by reduction of the focal methyl ester group with $LiAlH_4$.[10] The resulting benzyl alcohol moiety was etherified with propargyl bromide to obtain **2**. Subsequent removal of trityl groups yielded the discrete branched PEG hydrophilic block (**3**) (Scheme 1), as confirmed by MALDI-TOF mass spectroscopy ($M + Na^+$ = 1803 Da) (Figure 1) and NMR spectroscopy (Figure 11).

A series of PS with a narrow size distribution (PS**1**–**3**) was synthesized by conventional ATRP with (1-bromoethyl)benzene as an initiator.[23] PS**4**–**7** with high $Đ$ values ($Đ$ > 1.4) were synthesized via CuBr-catalyzed ATRP by adopting the temporal regulation of initiation proposed by Fors and co-workers.[19–22] The introduction of (1-bromoethyl)benzene at controlled rates to a mixture of the catalyst, ligand, and styrene monomers made the initiation temporally dispersed, which resulted in an increase of the $Đ$ of growing PS chains throughout Cu-ATRP process (Figures 2 and 3a). By adjusting the rate of initiator addition, we could synthesize PSs with desired $Đ$ values and molecular weights before the reaction reached completion (see Supporting Information for detailed conditions of

polymerization). The M_n and $Đ$ of PS**6** increased with time when the initiator addition rate was held constant (Figures 2a and 2b) at 90 ℃. In the case of PS**7**, the increase rate of $Đ$ was slower than that of M_n, which was ascribed to the higher reaction temperature (100 ℃), and the initiator addition rate was therefore increased (Figures 2c and 2d). This change in the addition rate resulted in a small additional peak in the gel permeation chromatography (GPC) spectrum (Figure 2c). Subsequent azidation of the bromide group at the chain end (Figure 3a) yielded a series of azido end-functionalized polystyrenes with different molecular weights and $Đ$ values (Table 1).

A series of branched-linear bPEG-PSs was synthesized by combining the hydrophilic branched PEG block and hydrophobic PS blocks by Cu(I)-catalyzed azide-alkyne cycloaddition (Scheme 1 and Figure 12). The $Đ$ values of bPEG-PS were lower than those of PS before conjugation (Table 1), which was ascribed to the fractionation of the high-molecular-weight BCPs during purification process to remove unreacted PS chains.

Scheme 1. Synthesis of a branched PEG hydrophilic block having three discrete PEG chains.

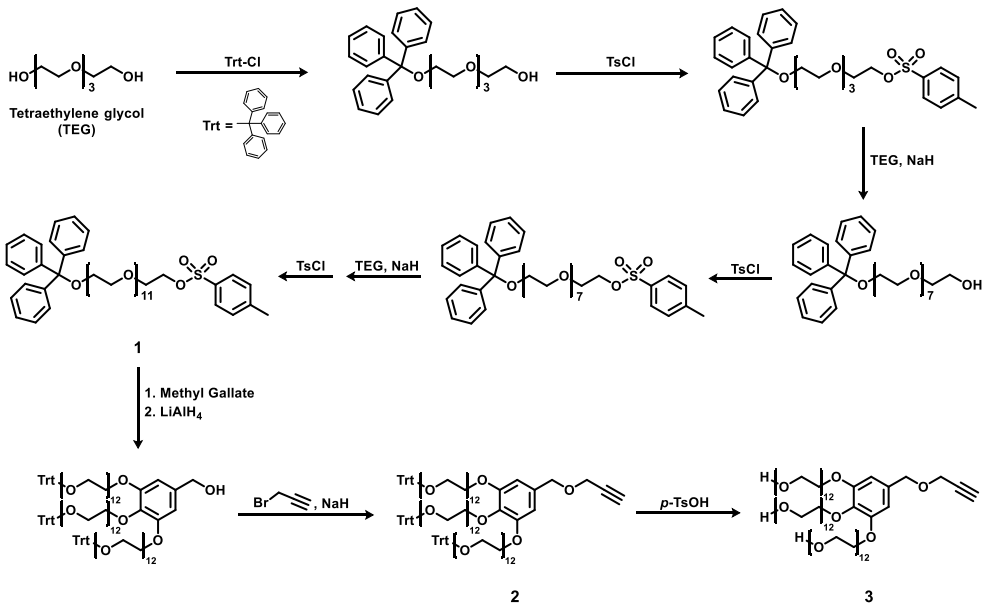

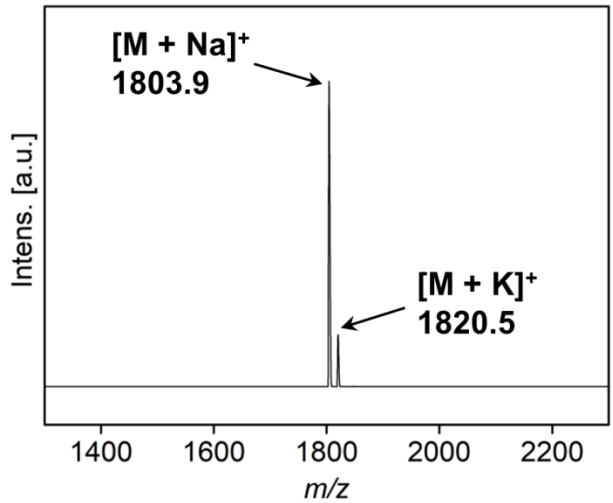

Figure 1. MALDI-TOF spectrum of **3**.

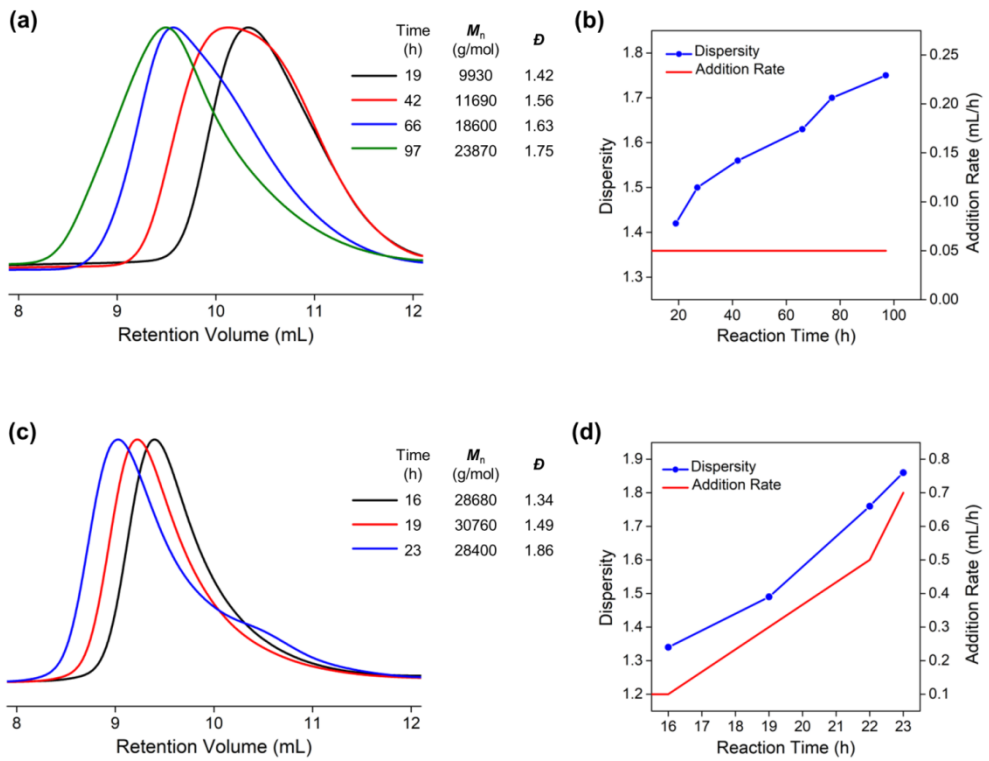

Figure 2. GPC profiles of (a) PS**6** and (c) PS**7** for different ATRP reaction times. (b, d) $Đ$ value and initiator addition (solution in anisole) rate as functions of time for (b) PS**6** and (d) PS**7**. M_n and $Đ$ were determined by GPC (DMF, 35 ℃, 1 mL/min) using PS standards.

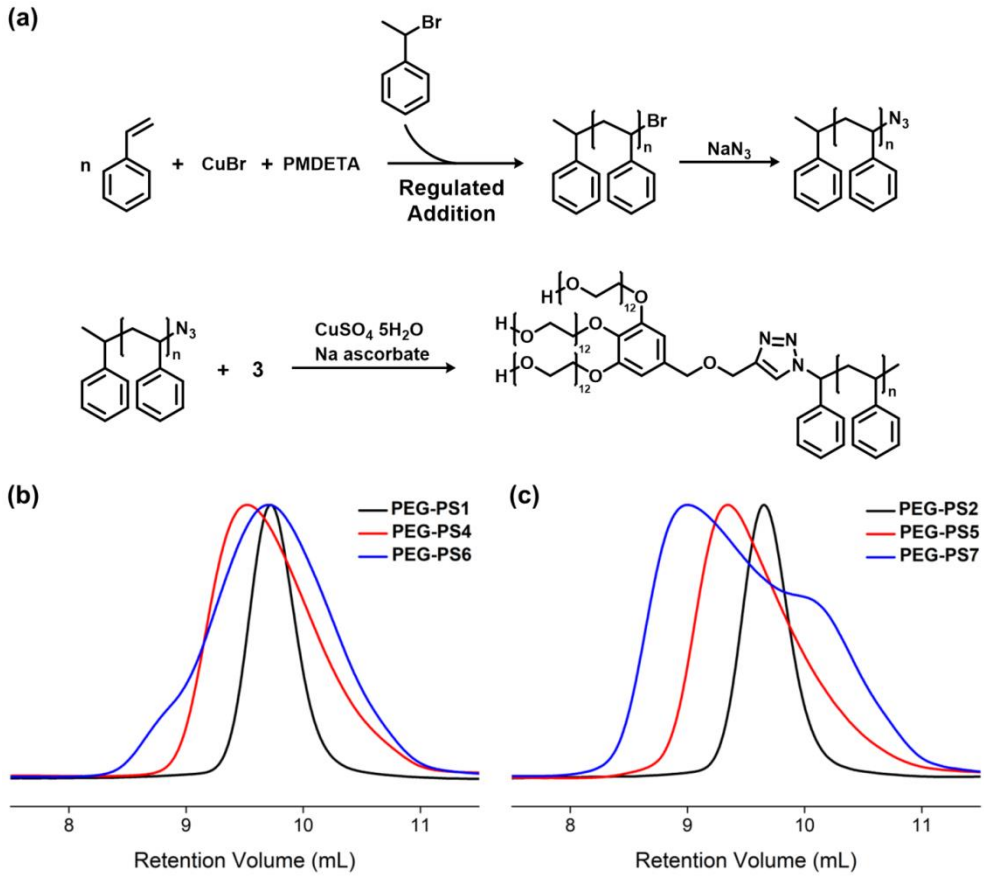

Figure 3. (a) Synthesis of azido end-functionalized PS with controlled $Đ$ via temporal regulation of initiation during ATRP and subsequent azidification followed by conjugation with **3** via CuAAC to obtain bPEG-PS. GPC (DMF) profiles of (b) bPEG-PS**1**, bPEG-PS**4**, and bPEG-PS**6**; (c) bPEG-PS**2**, bPEG-PS**5**, and bPEG-PS**7**.

Solution self-assembly of bPEG-PS performed using a solvent mixture.

We first investigated the self-assembly of bPEG-PS with the narrow-MWD hydrophobic PS block. To probe the effect of the MWD of the core-forming PS block on the self-assembly of bPEG-PS into bicontinuous cubic mesophases in solution, we self-assembled a series of bPEG-PS by the co-solvent method using a mixture of dioxane and acetone as a common solvent dissolving the BCPs. Water was added to the BCP solution at a slow rate (0.25 mL/h) via a syringe pump to reach a water content of 50 vol%, and the dispersion was dialyzed against water for 24 h to remove organic solvents. When only dioxane was used as a common solvent, bPEG-PS**1** (weight fraction of the PEG domain (w_{PEG}) = 6.0%), bPEG-PS**2** (w_{PEG} = 5.2%), and bPEG-PS**3** (w_{PEG} = 4.9%) all self-assembled to form polymer vesicles (average diameter measured by dynamic light scattering (DLS) = 530 nm) (Figures 4 and S4). Conversely, the disperse analog, $PEG550_3$-PS with a similar block ratio ($w_{PEG} \leq 6.2\%$) formed hexosomes under the same self-assembly conditions.[12] This morphological difference between bPEG-PSs with discrete PEG chains and disperse methoxy-PEG chains is presumed to arise from the difference in the end group of the PEG chains.

Table 1. GPC (DMF) profiles of PS and bPEG-PS.

Sample	M_n^{PS} (kg/mol)[a]	$Đ_{PS}$[a]	M_n (g/mol)[b]	$Đ$[b]	w_{PEG} (wt%)[c]
bPEG-PS**1**	22560	1.09	27100	1.09	6.0
bPEG-PS**2**	25650	1.11	31340	1.08	5.2
bPEG-PS**3**	27570	1.12	33690	1.07	4.9
bPEG-PS**4**	24750	1.41	26290	1.29	6.2
bPEG-PS**5**	27190	1.37	31650	1.32	5.2
bPEG-PS**6**	26340	1.57	26610	1.41	6.2
bPEG-PS**7**	34030	1.72	31880	1.61	5.1

[a]M_n^{PS}, $Đ_{PS}$ of azido end-functionalized polystyrenes, and [b]M_n, $Đ$ of bPEG-PS were determined by GPC (DMF, 35 °C, 1 mL min^{-1}) using PS standards. [c]The weight fraction of PEG (w_{PEG}) was calculated from the overall M_n and the molecular weight of PEG chains (546 g/mol for a single PEG chain).

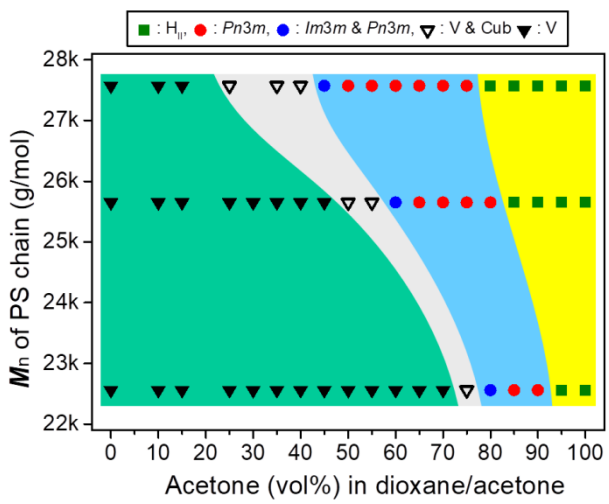

Figure 4. Phase diagram of the self-assembled morphologies of PEG-PS**1**, PEG-PS**2**, and PEG-PS**3** (from bottom to top) according to the composition of the common solvent mixture (Cub: cubosome, V: vesicle).

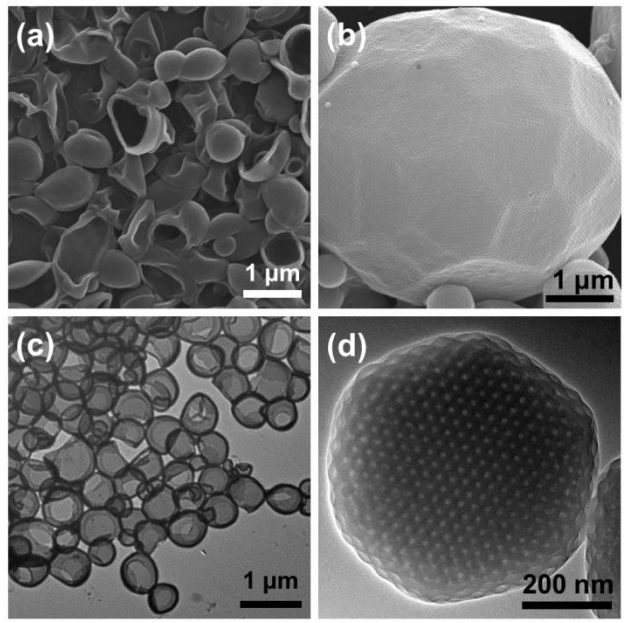

Figure 5. Representative SEM (a, b) and TEM (c, d) images of self-assembled bPEG-PS**1**. (a, c) SEM and TEM image of polymersomes of PEG-PS**1** self-assembled in acetone/dioxane (1:1, v/v). (b, d) SEM and TEM image of cubosomes of PEG-PS**1** self-assembled in acetone/dioxane (85:15, v/v).

The solubility parameter of the solvent mixture, which can be adjusted by changing the mixing ratio of two solvents with different solubility parameters, affects the conformation of the hydrophobic chain. In turn, this change in the chain conformation of the core-forming hydrophobic block induces the morphological transition of the self-assembled structure of a given BCP with a fixed block ratio. This simple method has been used to induce the morphological transition of the self-assembled structures of a single BCP from polymer vesicles to polymer cubosomes and hexosomes.

We screened the possible self-assembled morphologies of bPEG-PS**1** in solution using a mixture of acetone and dioxane as a common solvent dissolving the BCP. When the volume fraction of acetone was increased to ~75%, the self-assembled structure of bPEG-PS**1** changed from polymer vesicles to polymer cubosomes coexisting with polymer vesicles, while only polymer cubosomes were observed at acetone contents of 80–92 vol% (Figure 4, Table 1). The transformation from polymer vesicles to polymer cubosomes and then to hexosomes occurs as the BCP packing parameter increases from 1/3 to 1 or greater.[24] Our results indicated that an increase of the volume fraction of acetone in the solvent mixture makes the PS chain adopt a more compact conformation.

For the formation of polymer cubosomes of bPEG-PS**2** and bPEG-PS**3** with the higher-molecular-weight PS block, the volume fraction of acetone needed to obtain the same morphology decreased. Accordingly, an increase of acetone content had the increase of the molecular weight of PS in bPEG-PS. It can be assumed that because acetone is a relatively poor solvent for PS compared to dioxane, an increase of acetone content reduces the dimension of PS chains.[12] To compare the solubility of PS in acetone and in dioxane, we calculated the Hansen distance (R_a) of PS relative to these solvents as,

$$R_a = \sqrt{4(\delta_{d1} - \delta_{d2})^2 + (\delta_{p1} - \delta_{p2})^2 + (\delta_{h1} - \delta_{h2})^2}$$

where δ_d, δ_p, and δ_h are the dispersive, polar, and hydrogen bonding solubility parameters, respectively.[25,26] The Hansen solubility parameters for acetone are δ_d = 15.5 $MPa^{1/2}$, δ_p = 10.4 $MPa^{1/2}$, and δ_h = 6.95 $MPa^{1/2}$, while for dioxane, they are δ_d = 19.0 $MPa^{1/2}$, δ_p = 1.84 $MPa^{1/2}$, and δ_h = 7.36 $MPa^{1/2}$.[27] For polystyrene, these parameters are δ_d = 18.1 $MPa^{1/2}$, δ_p = 1.9 $MPa^{1/2}$, and δ_h = 2.8 $MPa^{1/2}$.[28] The $R_a^{acetone}$ and $R_a^{dioxane}$ of PS were calculated as 10.8 and 4.9, respectively. The smaller the

Hansen distance between two substances, the higher their solubility. As PS is less soluble in acetone than in dioxane, PS chain stretching is limited in the former solvent, and the chain dimension is therefore reduced, which leads to morphological transitions favoring structures with higher interfacial curvature.

In conclusion, simple adjustment of solvent composition allowed us to induce a morphological transition of a BCP corresponding to the block ratio change of a block copolymer without changing the BCP structure. By using acetone and dioxane mixtures of different compositions as the common solvent, we could observe the formation of a wide range of morphologies from vesicles to hexosomes from a single bPEG-PS and concluded that the adjustment of the solvent solubility parameter of the solvent is a useful tool for screening the possible morphologies produced by the self-assembly of BCPs in solution.

Effect of $Đ$ of the hydrophobic PS block on the self-assembly of bPEG-PS in solution.

To investigate the effect of hydrophobic chain $Đ$ on the self-assembly of BCPs, a series of bPEG-PSs with similar M_n, but different $Đ$ values was self-assembled (Figures 3b and 3c). A representative BCP with a narrow MWD in the hydrophobic PS block, bPEG-PS**1** (M_n = 27100, $Đ$ = 1.09), self-assembled to form polymer cubosomes when the acetone/dioxane mixture (acetone = 80–92 vol%) was used as a common solvent (Figures 4, 5, and 6a–6c). The cubosomes of bPEG-PS**1** showed $Pn\bar{3}m$ symmetry according to small-angle X-ray scattering (SAXS) analysis (Figure 7a). In contrast, cubosomes self-assembled from bPEG-PS**4** (M_n = 26290, $Đ$ = 1.29) showed $Im\bar{3}m$ symmetry (Figures 6d–6f and 7b) according to SAXS and fast Fourier transform (FFT) analyses,[29] and only sponge phases (L_3) formed when the acetone content was lower than 95 vol% (Figures 6c and 9a). It is worth mentioning that the lattice constants calculated by FFT analysis match those calculated by SAXS analysis (Figures 6, 7 and 8). When bPEG-PS**6** (M_n = 26610, $Đ$ = 1.41) was self-assembled, only the sponge phase was observed regardless of acetone content (Figures 6g, 6h, and 9a). Based on SEM/TEM images and SAXS spectra, we concluded that the internal order of the self-assembled morphologies deteriorated with increasing $Đ$ (Figures 6 and 8). It is worth mentioning that the lattice constants calculated by FFT analysis match those calculated by SAXS analysis (Figures 6, 7 and 8).

The above deterioration of the order of the internal cubic phases with increasing $Đ$ of the PS block was also observed for the self-assembly of bPEG-PS**2**, bPEG-PS**5**, and bPEG-PS**7**. Cubosomes were obtained in the self-assembly of bPEG-PS**2** (M_n = 31340, $Đ$ = 1.08) and bPEG-PS**5** (M_n = 31650, $Đ$ = 1.32) (Figures 7c, 7d, 8,

and 9b), while bPEG-PS**7** (M_n = 31880, $Đ$ = 1.61) self-assembled to form sponge phases (L_3) only (Figures 8g, 8h, and 9b). Interestingly, as $Đ$ increased from 1.1 to 1.3, the dominant symmetry of self-assembled cubosomes changed from $Pn\bar{3}m$ (Figure 7a and 7c) to $Im\bar{3}m$ (Figures 7b and 7d). For the self-assembly of bPEG-PS**1**–**3**, $Im\bar{3}m$ symmetry was only observed mixed with $Pn\bar{3}m$ symmetry within a narrow range of acetone content as indicated by the results of FFT and SAXS analyses (Figures 4 and S5). However, only $Im\bar{3}m$ was observed for cubosomes self-assembled from bPEG-PS**4** and bPEG-PS**5** (Figures 6f, 7b and 7d). As species of the $Im\bar{3}m$ symmetry have a smaller interfacial curvature than those of $Pn\bar{3}m$ symmetry,[30–32] this internal lattice change of polymer cubosomes might be attributed to the reduced interfacial curvature arising from the increased MWD of the PS block. The morphological changes of decreased-interfacial-curvature structures with increasing $Đ$ in the major block of block copolymers have been previously observed for the self-assembly of block copolymers in the bulk.[1,4]

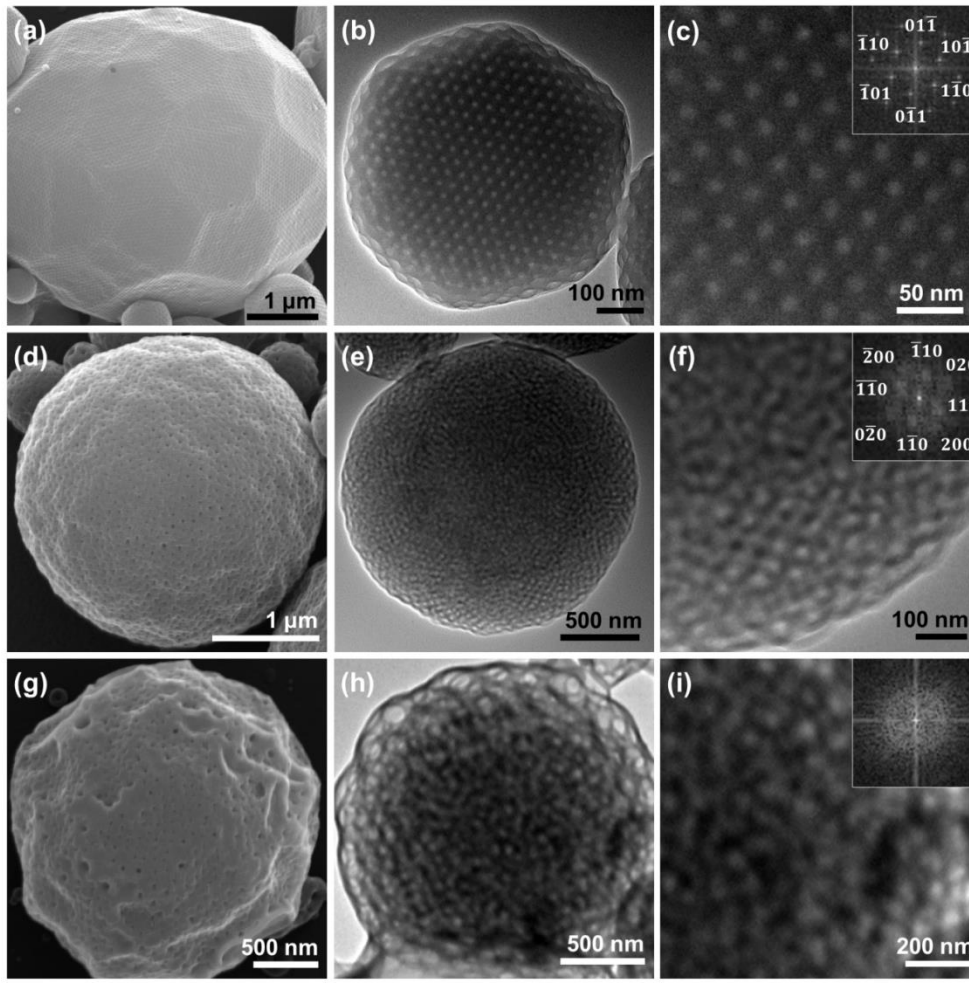

Figure 6. Representative SEM and TEM images of cubosomes of (a–c) bPEG-PS**1** ($Đ$ = 1.09, acetone content = 85 vol%, $Pn\bar{3}m$, lattice constant = 40 nm), (d–f) bPEG-PS**4** ($Đ$ = 1.29, acetone content = 95 vol%, $Im\bar{3}m$, lattice constant = 67 nm), and (g, h) bPEG-PS**6** ($Đ$ = 1.41, acetone content = 100 vol%). (c), (f), and (i) are magnified images of (b) and (e), respectively, with the fast Fourier transform (FFT) images shown in the insets. Cubosomes were viewed along the [111] direction in (c), and along the [100] direction in (f). The lattice constants were calculated by FFT analysis using ImageJ software.

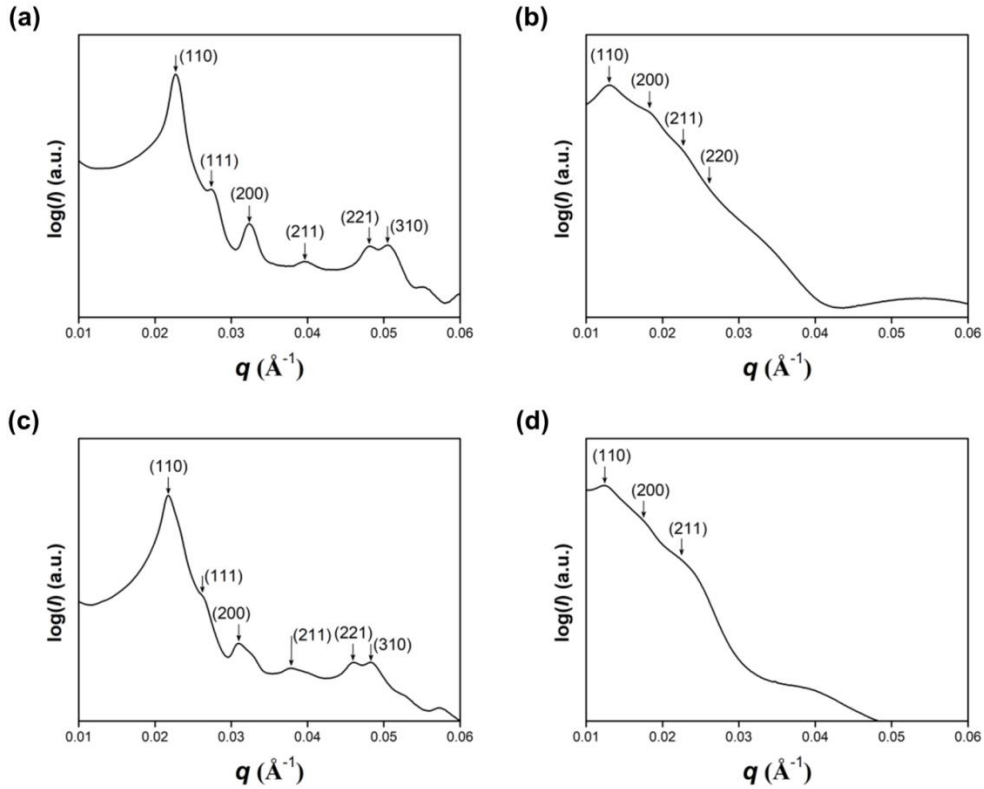

Figure 7. Representative SAXS spectra of cubosomes of self-assembled bPEG-PS. (a) bPEG-PS**1** ($Đ$ = 1.09, acetone content = 85 vol%, $Pn\bar{3}m$, lattice constant = 39 nm), (b) bPEG-PS**4** ($Đ$ = 1.29, acetone content = 95 vol%, $Im\bar{3}m$, lattice constant = 68 nm), (c) bPEG-PS**2** ($Đ$ = 1.08, acetone content = 70 vol%, $Pn\bar{3}m$, lattice constant = 42 nm), and (d) bPEG-PS**5** ($Đ$ = 1.32, acetone content = 70 vol%, $Im\bar{3}m$, lattice constant = 72 nm).

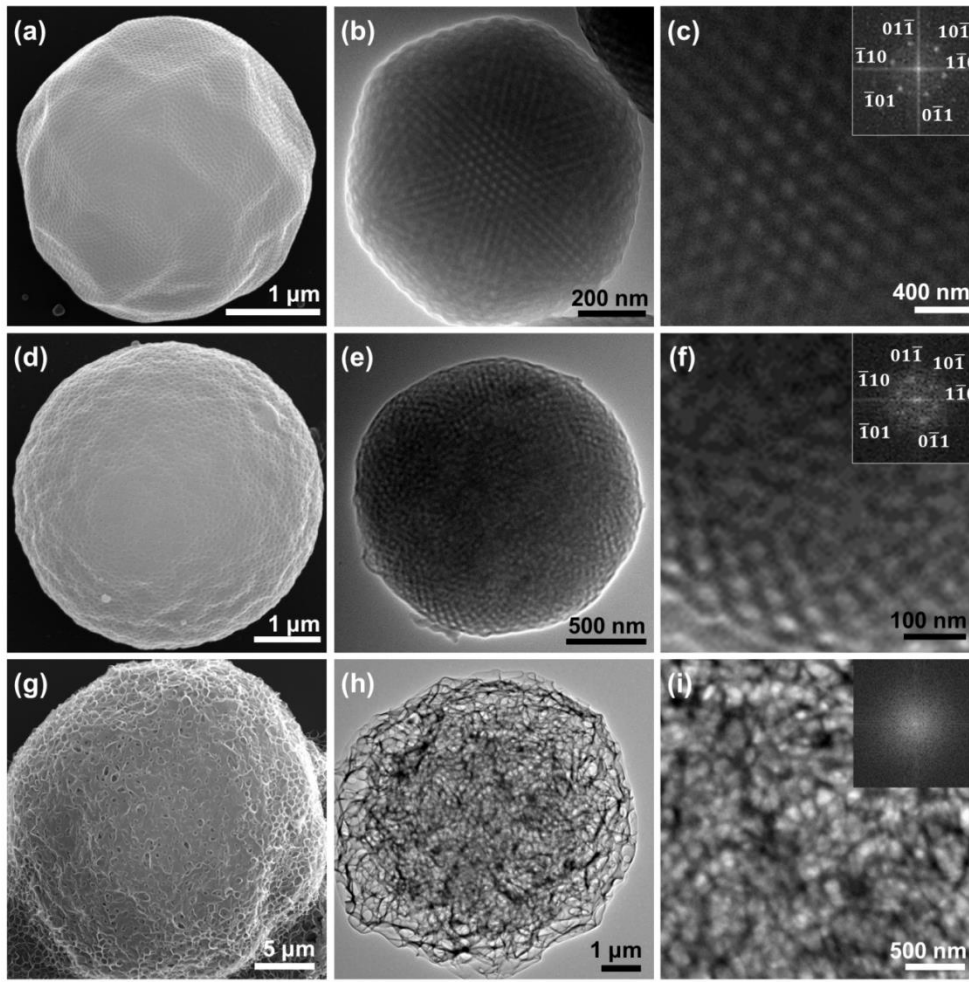

Figure 8. Representative SEM and TEM images of cubosomes of (a–c) bPEG-PS**2** ($Đ$ = 1.08, acetone content = 70 vol%, $Pn\bar{3}m$, lattice constant = 41 nm), (d–f) bPEG-PS**5** ($Đ$ = 1.32, acetone content = 70 vol%, $Im\bar{3}m$, lattice constant = 73 nm), and (g, h) bPEG-PS**7** ($Đ$ = 1.61, acetone content = 70%). (c), (f), and (i) are magnified images of (b) and (e), respectively, with the fast Fourier transform (FFT) images shown in the insets. Cubosomes in TEM images were viewed along the [111] direction. The lattice constants were calculated by FFT analysis using ImageJ software.

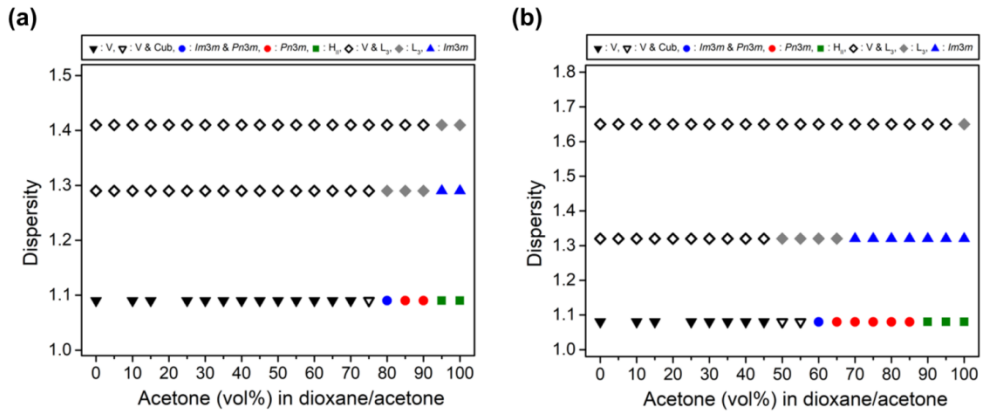

Figure 9. (a) Phase diagram of bPEG-PS**1** ($Đ$ = 1.09), bPEG-PS**4** ($Đ$ = 1.29), and bPEG-PS**6** ($Đ$ = 1.41). (b) Phase diagram of bPEG-PS**2** ($Đ$ = 1.08), bPEG-PS**5** ($Đ$ = 1.32), and bPEG-PS**7** ($Đ$ = 1.61). (V: vesicle, Cub: cubosome)

III. CONCLUSION

The effect of the MWD of core-forming hydrophobic blocks on the self-assembled structures of BCPs in solution was investigated using BCPs comprising a branched poly(ethylene glycol) (bPEG) hydrophilic block with a discrete molecular weight and a hydrophobic polystyrene (PS) block with the desired MWD. A series of bPEG-PSs with similar M_ns but different $Đ$ values was self-assembled using acetone/dioxane mixtures as the common solvent, with the concentration of acetone corresponding to the PS block ratio. The increase of $Đ$ resulted in a gradual deterioration of the internal order of bPEG-PS polymer cubosomes from a cubic crystalline phase to a disordered cubic and sponge phases. In addition, increasing $Đ$ of the core-forming hydrophobic PS block of bPEG-PS from 1.1 to 1.3 while its M_n remained constant caused a morphological change in the symmetry of the self-assembled cubosomes from $Pn\bar{3}m$ to $Im\bar{3}m$. Our results suggest that the major parameter responsible for the increased disorder and the morphological change of the internal structure of polymer cubosomes is the MWD of the core-forming hydrophobic block.

IV. Experimental Section

Materials

Unless otherwise stated, all reactions were carried out under N_2 atmosphere. All reagents and chemicals were purchased from Sigma Aldrich, Alfa Aesar and TCI and used as received. Styrene (99+%) was purchased from Sigma Aldrich and filtered over a column of basic alumina before use. Dry solvents were obtained via distillation using Na and benzophenone as drying agents for tetrahydrofuran (THF), and using CaH_2 for dichloromethane (DCM).

General Information

^{1}H NMR spectra were recorded on Agilent 400-MR DD2 magnetic resonance system and Varian/Oxford As-500 using CD_2Cl_2 or $CDCl_3$ as solvents. Molecular weights of polymers were measured on Agilent 1260 infinity gel permeation chromatography (GPC) system equipped with a PL gel 5 μm mixed D column and differential refractive index detectors. DMF was used as an eluent with a flow rate of 1 mL min^{-1} at 35 ℃. A PS standard kit (Agilent Technologies) was used for calibration. Matrix-assisted laser desorption/ionization time-of-flight mass spectrometry (MALDI-TOF-MS) was performed on Bruker Ultraflex II TOF/TOF mass spectrometer equipped with a nitrogen laser (335 nm). The analytical sample was prepared by mixing a THF solution of an analyte with a THF solution of sinapic acid.

Scanning electron microscopy (SEM) was performed on Hitachi S-4300 at an acceleration voltage of 15 kV. Typically, dried samples were placed on a conductive carbon tape and then sputtered with Pt with a thickness of 3 nm by

using Hitachi E-1030 ion sputter. Transmission electron microscopy (TEM) was performed on JEOL JEM-2100 microscope at 200 kV. Specimens were prepared by placing a drop of the sample solution on a carbon-coated Cu grid (200 mesh, EM science) and then air-drying the grid.

Synchrotron small angle X-ray scattering (SAXS) data were obtained on 6D SAXS beam line at Pohang acceleration laboratory in Korea (PLS-II, 3.0 GeV). The sample-to-detector distance was 3.5 m. Ti-SBA-15 was used as standard sample and scattering spectra were taken in a transmission mode at room temperature (11.6 keV).

ImageJ software (https://imagej.nih.gov/ij/) was used to conduct 2D fast Fourier transform (FFT) on TEM images. Lattice constants of polymer cubosomes were calculated from the FFT images.

Synthesis of a discrete heterobifunctional PEG (Trt-PEG$_{12}$-Ts)

The following procedure was adapted from the previously published literature.[17,18] Compound **1** was obtained as a mixture with dityrityl by-products. The mixture was used in the next step without further purification as the by-products are unreacting. The amount of compound **1** in the mixture was determined from ^{1}H NMR analysis (Figure 10).

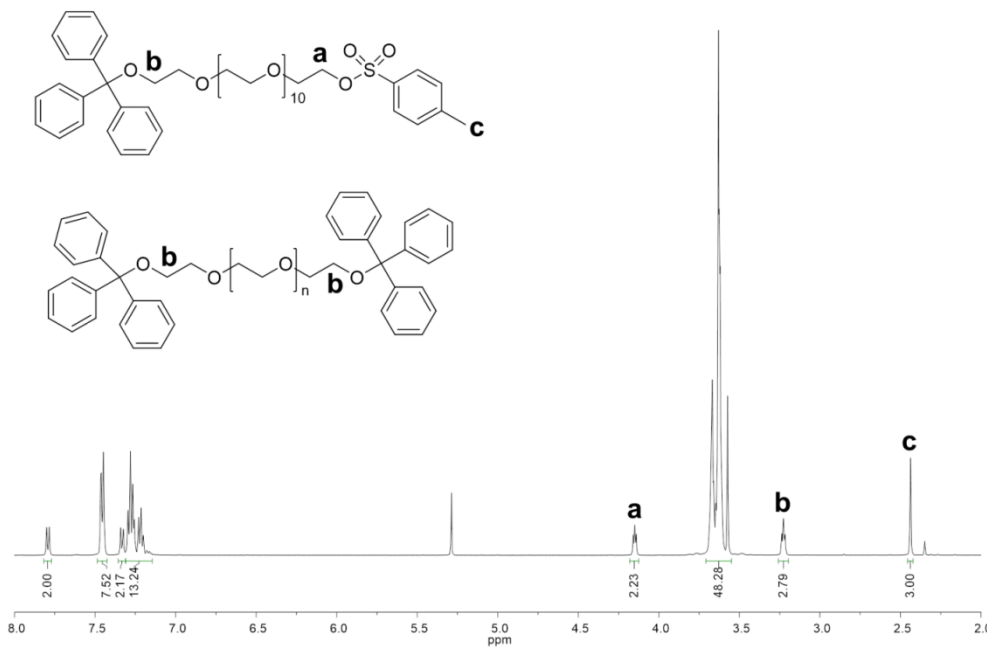

Figure 10. ^{1}H NMR spectrum (400 MHz, $CDCl_3$) of Trt-PEG$_{12}$-Ts (crude).

Synthesis of a discrete hydrophilic PEG block (3)

Methyl gallate (0.195 g, 1.06 mmol) and K_2CO_3 (1.17 g, 8.48 mmol) were added to the 500 mL two-neck flask charged with acetone under N_2. The crude mixture from

the previous step (6.93 g) containing compound **1** (less than 3.30 g, 3.50 mmol) was added to the flask, and the solution was refluxed at 75 ℃ for 12 h. The reaction was monitored by MALDI-TOF. Additional amount of the polyethylene glycol reactant mixture was added until the reaction was complete. After the complete consumption of the methyl gallate was confirmed on MALDI-TOF, the reaction was cooled at room temperature. The crude mixture was filtered through a filter paper and the solvent was evaporated under reduced pressure. The residue was extracted with DCM and washed with brine three times. The organic phase was dried over anhydrous Na_2SO_4 and the solvent was removed under reduced pressure.

Without further purification, the crude mixture containing **2** (less than 1.06 mmol) was reduced with $LiAlH_4$ (80 mg, 2.12 mmol) in THF under N_2 atmosphere for 3 h. The reduction yielded crude product which was purified by column chromatography on silica (DCM/MeOH, 20/1 to 10/1, v/v) to obtain compound **3** as a pale yellow liquid (2.30 g, 0.932 mmol, 88% over 2 steps). ^{1}H NMR (δ = ppm, 400 MHz, $CDCl_3$) 7.44 (d, 15H, *J* = 8 Hz), 7.30-7.17 (m, 36H), 6.61 (s, 2H), 4.54 (d, 2H, *J* = 8 Hz), 4.14 (t, 4H, 8 Hz), 4.10 (t, 2H, 4 Hz), 3.81 (t, 4H, *J* = 8 Hz), 3.75 (t, 2H, *J* = 4 Hz), 3.70-3.57 (m, -CH_2CH_2O-), 3.21 (t, 6H, *J* = 4 Hz).

Compound **3** (2.30 g, 0.932 mmol) was dissolved in dry THF (25 mL) and the solution was added dropwise to a suspension of NaH (60% suspension in oil, 44.7 mg, 1.86 mmol) in dry THF at 0 ℃ under N_2 atmosphere, and the mixture was stirred from 0 ℃ to room temperature for 2 h. Propargyl bromide (0.166 g, 1.40 mmol) was added to the reaction mixture and stirred at room temperature for 12 h. The reaction mixture was cooled to 0 ℃ and saturated NH_4Cl solution was added. After evaporating THF under reduced pressure, the mixture was extracted with

DCM, washed with brine and dried over anhydrous Na_2SO_4. The crude product was used in the next step without further purification.

To a solution of crude mixture containing **4a** (less than 0.932 mmol) in DCM/MeOH (1/1, v/v) was added *p*-toluene sulfonic acid monohydrate (0.605 g, 3.18 mmol), and the mixture was stirred at room temperature for 2.5 h. The reaction mixture was concentrated under reduced pressure, and the residue was extracted with DCM. The organic phase was washed with a saturated $NaHCO_3$ aqueous solution (10 mL) and brine (10 mL), and dried over anhydrous Na_2SO_4. The crude product was purified by column chromatography on silica (DCM/MeOH, 9/1, v/v) to obtain compound **4b** as a slightly yellow liquid (1.41 g, 0.792 mmol, 85% over 2 steps). ^{1}H NMR (δ = ppm, 400 MHz, $CDCl_3$) 6.59 (s, 2H), 4.49 (s, 2H), 4.15 (m, 6H), 4.11 (t, 2H, 4 Hz), 3.83 (t, 4H, *J* = 4 Hz), 3.77 (t, 2H, *J* = 4 Hz), 3.74-3.58 (m, -CH_2CH_2O-), 2.49 (t, 1H, *J* = 4 Hz).

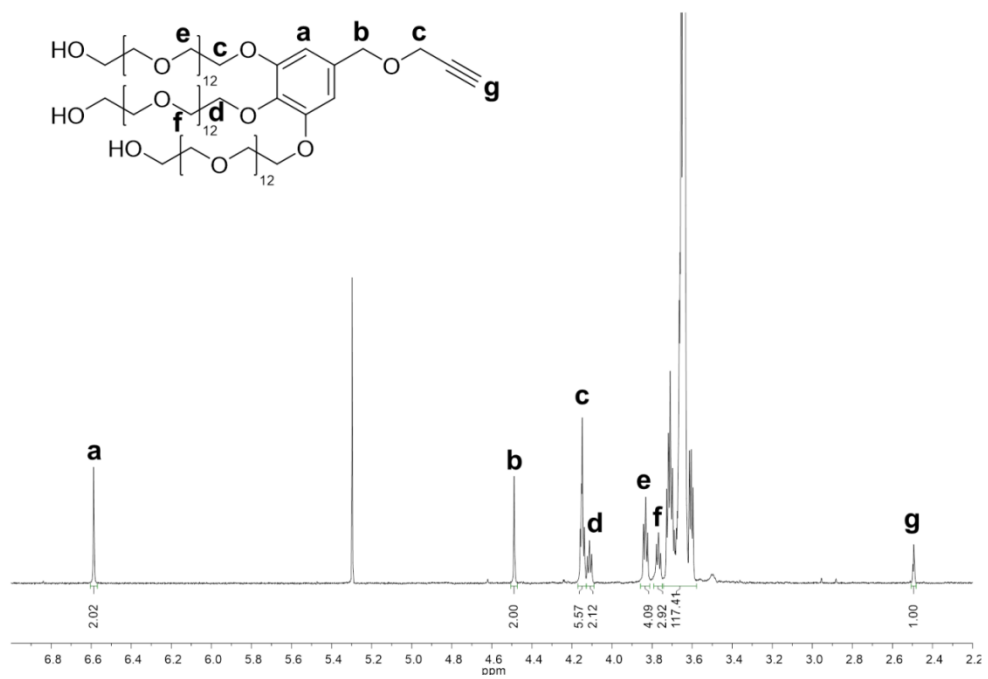

Figure 11. ^{1}H NMR spectrum (400 MHz, $CDCl_3$) of **3**.

General procedure for the synthesis of azido end-functionalized polystyrenes with narrow Đ

CuBr (313 mg, 2.2 mmol) was charged in a 100 mL Schlenk flask and dried under vacuum for 15 min. *N,N,N',N'',N''*-pentamethyldiethylenetriamine (PMDETA) (0.91 mL, 4.4 mmol) dissolved in anisole (2 mL) was added, and the mixture was gently stirred under N_2 for 10 min. (1-Bromoethyl)benzene (80 mg, 0.44 mmol) in anisole (1 mL) and styrene (50 mL, 440 mol) was added to the mixture and was degassed via bubbling N_2 into the mixture for 15 min. ATRP reaction was carried out at 90 ℃. The reaction was monitored by GPC and quenched by exposing the mixture to air and cooling it in liquid N_2 bath. The cooled mixture was filtered through a pad of aluminum oxide (basic) using DCM as an eluent for removal of Cu ions. The filtered solution was concentrated by rotary evaporation, diluted with a small amount of DCM and then precipitated into methanol. Polystyrene end-functionalized with bromine was obtained as white powder by filtration and dried in vacuo.

The obtained bromo end-functionalized polystyrene (10 g, ca. 0.44 mmol, 1 eq.) and sodium azide (0.283 g, 10 eq.) were dissolved in DMF (250 mL) and stirred at room temperature under N_2 for 12 h. DMF was removed by rotary evaporation and azido end-functionalized polystyrene was precipitated into methanol.

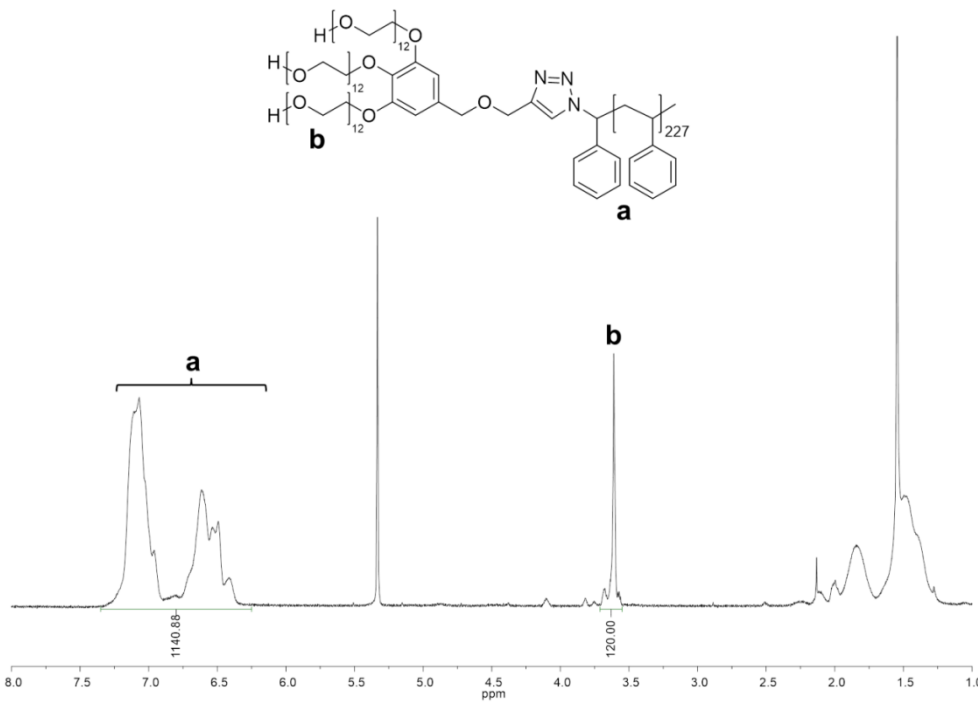

Figure 12. ^{1}H NMR spectrum (400 MHz, $CDCl_3$) of bPEG-PS**1**.

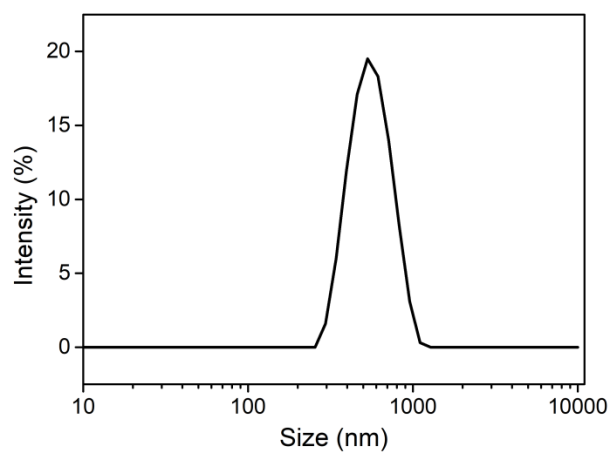

Figure 13. DLS spectrum of the self-assembled vesicles of bPEG-PS**1** (average diameter = 530 nm) using dioxane as the common solvent.

General procedure for the synthesis of azido end-functionalized polystyrenes with high Đ

CuBr (194 mg, 1.4 mmol) was charged in a 50 mL Schlenk flask and dried under vacuum for 1 h. *N*,*N*,*N'*,*N''*,*N''*-pentamethyldiethylenetriamine (PMDETA) (0.42 mL, 2.0 mmol) was dissolved in anisole (2 mL) in a sealed vial under N_2, degassed via bubbling N_2 into the mixture for 15 min, and the solution was transferred to the Schlenk flask containing CuBr under N_2. Styrene (47 mL, 409 mmol) was charged in a 50 mL Schlenk flask under N_2, degassed via bubbling N_2 for 15 min and was added to the mixture of CuBr and PMDETA. The initiator, (1-Bromoethyl)benzene (62.5 mg, 1.7 mmol), was dissolved in anisole (5 mL) in a sealed vial under N_2, degassed via bubbling N_2 for 15 min, and was filled into a 6 mL syringe. The initiator was added to the flask containing CuBr, PMDETA, and styrene during ATRP reaction via syringe pump at 90–100 ℃. The addition rate of the initiator was controlled while monitoring the progress of the reaction by GPC. When the growing polymer reached the desired M_n and $Đ$, the polymerization was quenched by exposing the mixture to air and cooling it in liquid N_2 bath. The cooled mixture was filtered through a pad of aluminum oxide (basic) using DCM as an eluent for removal of Cu ions. The filtered solution was concentrated by rotary evaporation, diluted with a small amount of DCM and then precipitated into methanol. Polystyrene end-functionalized with bromine was obtained as white powder by filtration and dried in vacuo. Azido end-functionalized polystyrene was obtained following the same procedure as described above.

The obtained bromo end-functionalized polystyrene (10 g, ca. 0.435 mmol, 1 eq.) and sodium azide (0.283 g, 10 eq.) were dissolved in DMF (250 mL) and stirred at room temperature under N_2 for 12 h. DMF was removed by rotary evaporation and azido end-functionalized polystyrene was precipitated into methanol.

Table 2. GPC (DMF) profiles of PS**4** at each reaction time during ATRP.

Time (h)	M_n (g/mol)[a]	$Đ$[a]	Addition Rate (mL/h)[b]
2	8100	1.24	0.5
3	15620	1.32	0.6
4	20000	1.39	0.7
5	23370	1.40	0.8

Table 3. GPC (DMF) profiles of PS**5** at each reaction time during ATRP.

Time (h)	M_n (g/mol)[a]	$Đ$[a]	Addition Rate (mL/h)[b]
3	7160	1.23	0.5
5	13460	1.30	0.5
6	16790	1.33	0.5
8	24110	1.37	0.5
9	25870	1.38	0.5

Table 4. GPC (DMF) profiles of PS**6** at each reaction time during ATRP.

Time (h)	$\boldsymbol{M}_n$ (g/mol)[a]	$\boldsymbol{Đ}$[a]	Addition Rate (mL/h) [b]
19	9930	1.42	0.05
27	11080	1.50	0.05
42	11690	1.56	0.05
66	18600	1.63	0.05
77	19670	1.70	0.05
97	23870	1.75	0.05

Table 5. GPC (DMF) profiles of PS**7** at each reaction time during ATRP.

Time (h)	$\boldsymbol{M}_n$ (g/mol)[a]	$\boldsymbol{Đ}$[a]	Addition Rate (mL/h) [b]
16	28680	1.34	0.1
19	30760	1.49	0.3
22	29520	1.76	0.5
23	28400	1.86	0.7

[a]M_n and $Đ$ were determined by GPC (DMF, 35 ℃, 1 mL/min) using PS standards.

[b]The volume refers to the volume of the initiator solution in anisole.

General procedure for the conjugation of the hydrophilic block and the polystyrenes

The discrete hydrophilic block and the polystyrenes were coupled via Cu-catalyzed azide-alkyne Huisgen cycloaddition (CuAAC). Compound **4** (30 mg, 0.017 mmol), azido end-functionalized polystyrene (2.5 equivalents of compound **4**), $CuSO_4 \cdot 5H_2O$ (13 mg, 0.052 mmol), and sodium ascorbate (7 mg, 0.035 mmol) were dissolved in dry DMF under N_2 atmosphere. The mixture was stirred for 3 h at room temperature. After confirming via GPC that compound **4** were exhausted, DMF was removed by rotary evaporation. The excess unreacted polystyrene was removed by column chromatography on silica (EA/Hexane 1/1, v/v) and the desired product, bPEG-PS, was collected (DCM/MeOH, 9/1, v/v). The product was precipitated into methanol to obtain pure bPEG-PS in white powder.

General procedure for the self-assembly of bPEG-PS in solution

The synthesized bPEG-PS was self-assembled following the method used in our previous studies.[10–14] 5 mg of bPEG-PS was dissolved in 1 mL of acetone/dioxane solvent mixture followed by the addition of water at the rate of 0.25 mL/h for 4 h. The organic solvent was removed by subsequent dialysis against water for 24 h.

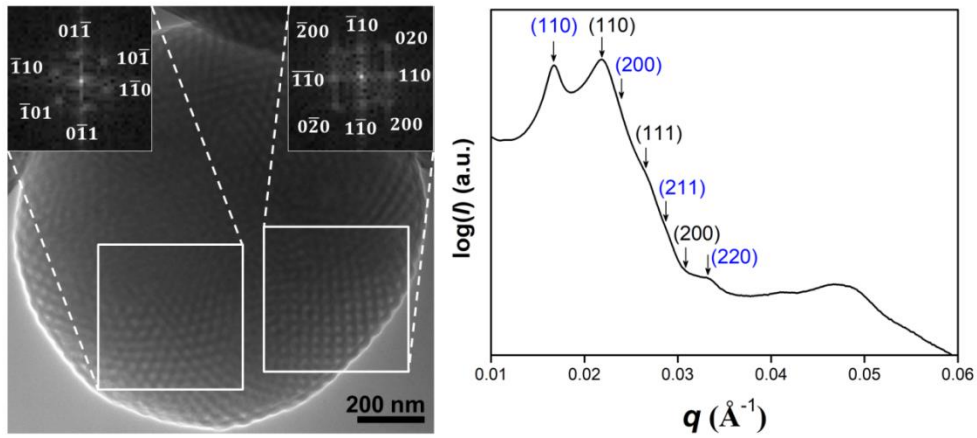

Figure 14. TEM image (left) and SAXS spectrum (right) of the self-assembled cubosome of bPEG-PS**1** (acetone content = 82 vol%). Miller indices in the SAXS spectrum correspond to expected Bragg peak positional ratios (blue: $Im\bar{3}m$, black: $Pn\bar{3}m$).

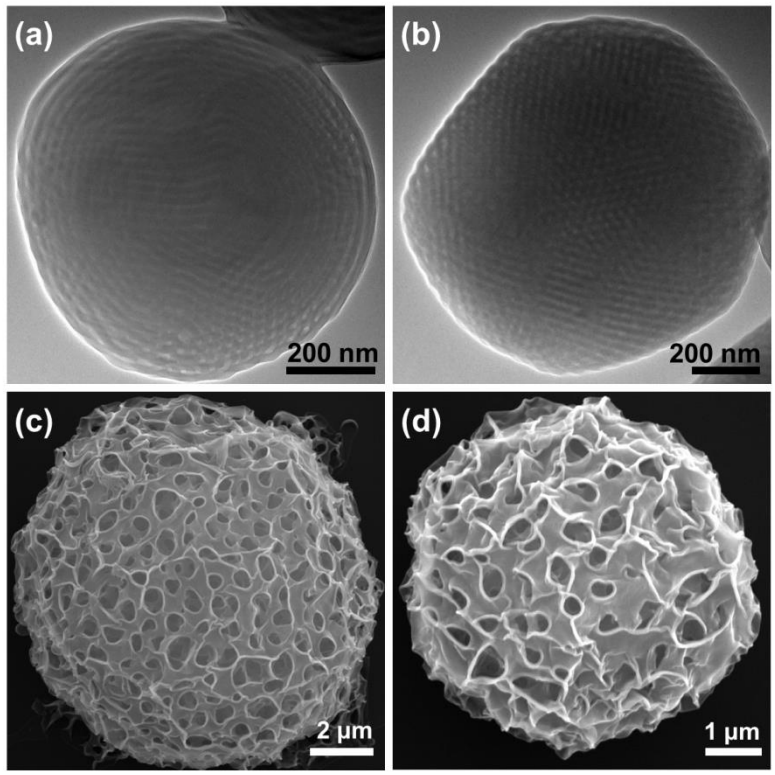

Figure 15. (a, b) TEM images of (a) a hexosome of bPEG-PS**1** (acetone content = 95 vol%) and (b) a cubosome of bPEG-PS**3** (acetone content = 45%). (c, d) SEM images of sponge phases of (c) bPEG-PS**4** ($Đ$ = 1.29, acetone content = 80 vol%) and (d) bPEG-PS**5** ($Đ$ = 1.32, acetone content = 60 vol%).

REFERENCES

(1) Lynd, N. A.; Hillmyer, M. A. Influence of Polydispersity on the Self-Assembly of Diblock Copolymers. *Macromolecules* **2005**, *38*, 8803–8810.

(2) Lynd, N. A.; Hamilton, B. D.; Hillmyer, M. A. The role of polydispersity in the lamellar mesophase of model diblock copolymers. *J. Polym. Sci. B* **2007**, *45*, 3386–3393.

(3) Lynd, N. A.; Hillmyer, M. A. Effects of Polydispersity on the Order−Disorder Transition in Block Copolymer Melts. *Macromolecules* **2007**, *40*, 8050–8055.

(4) Lynd, N. A.; Meuler, A. J.; Hillmyer, M. A. Polydispersity and block copolymer self-assembly. *Prog. Polym. Sci.* **2008**, *33*, 875–893.

(5) Terreau, O.; Luo, L.; Eisenberg, A. Effect of Poly(acrylic acid) Block Length Distribution on Polystyrene-b-Poly(acrylic acid) Aggregates in Solution. 1. Vesicles. *Langmuir* **2003**, *19*, 5601–5607.

(6) Jiang, Y.; Chen, T.; Ye, F.; Liang, H.; Shi, A.-C. Effect of Polydispersity on the Formation of Vesicles from Amphiphilic Diblock Copolymers. *Macromolecules* **2005**, *38*, 6710–6717.

(7) Terreau, O.; Bartels, C.; Eisenberg, A. Effect of Poly(acrylic acid) Block Length Distribution on Polystyrene-b-poly(acrylic acid) Block Copolymer Aggregates in Solution. 2. A Partial Phase Diagram. *Langmuir* **2004**, *20*, 637–645.

(8) Li, X.; Tang, P.; Qiu, F.; Zhang, H.; Yang, Y. Aggregates in Solution of Binary Mixtures of Amphiphilic Diblock Copolymers with Different Chain Length. *J. Phys. Chem. B* **2006**, *110*, 2024–2030.

(9) Das, A.; Petkau-Milroy, K.; Klerks, G.; van Genabeek, B.; Lafleur, R. P. M.; Palmans, A. R. A.; Meijer, E. W. Consequences of Dispersity on the Self-Assembly

of ABA-Type Amphiphilic Block Co-Oligomers. *ACS Macro Lett.* **2018**, *7*, 546–550.

(10) La, Y.; Park, C.; Shin, T. J.; Joo, S. H.; Kang, S.; Kim, K. T. Colloidal inverse bicontinuous cubic membranes of block copolymers with tunable surface functional groups. *Nat. Chem.* **2014**, *6*, 534–541.

(11) An, T. H.; La, Y.; Cho, A.; Jeong, M. G.; Shin, T. J.; Park, C.; Kim, K. T. Solution Self-Assembly of Block Copolymers Containing a Branched Hydrophilic Block into Inverse Bicontinuous Cubic Mesophases. *ACS Nano* **2015**, *9*, 3084–3096.

(12) La, Y.; An, T. H.; Shin, T. J.; Park, C.; Kim, K. T. A Morphological Transition of Inverse Mesophases of a Branched-Linear Block Copolymer Guided by Using Cosolvents. *Angew. Chem. Int. Ed.* **2015**, *54*, 10483–10487.

(13) Park, C.; La, Y.; An, T. H.; Jeong, H. Y.; Kang, S.; Joo, S. H.; Ahn, H.; Shin, T. J.; Kim, K. T. Mesoporous monoliths of inverse bicontinuous cubic phases of block copolymer bilayers. *Nat. Commun.* **2015**, *6*, 6392.

(14) Cho, A.; La, Y.; Shin, T. J.; Park, C.; Kim, K. T. Structural Requirements of Block Copolymers for Self-Assembly into Inverse Bicontinuous Cubic Mesophases in Solution. *Macromolecules* **2016**, *49*, 4510–4519.

(15) Lin, Z.; Liu, S.; Mao, W.; Tian, H.; Wang, N.; Zhang, N.; Tian, F.; Han, L.; Feng, X.; Mai, Y. Tunable Self-Assembly of Diblock Copolymers into Colloidal Particles with Triply Periodic Minimal Surfaces. *Angew. Chem. Int. Ed.* **2017**, *56*, 7135–7140.

(16) Lyu, X.; Xiao, A.; Zhang, W.; Hou, P.; Gu, K.; Tang, Z.; Pan, H.; Wu, F.; Shen, Z.; Fan, X.-H. Head–Tail Asymmetry as the Determining Factor in the

Formation of Polymer Cubosomes or Hexasomes in a Rod–Coil Amphiphilic Block Copolymer. *Angew. Chem. Int. Ed.* **2018**, *57*, 10132–10136.

(17) Wawro, A. M.; Muraoka, T.; Kinbara, K. Chromatography-free synthesis of monodisperse oligo(ethylene glycol) mono-p-toluenesulfonates and quantitative analysis of oligomer purity. *Polym. Chem.* **2016**, *7*, 2389–2394.

(18) Wawro, A. M.; Muraoka, T.; Kato, M.; Kinbara, K. Multigram chromatography-free synthesis of octa(ethylene glycol) p-toluenesulfonate. *Org. Chem. Front.* **2016**, *3*, 1524–1534.

(19) Gentekos, D. T.; Dupuis, L. N.; Fors, B. P. Beyond Dispersity: Deterministic Control of Polymer Molecular Weight Distribution. *J. Am. Chem. Soc.* **2016**, *138*, 1848–1851.

(20) Kottisch, V.; Gentekos, D. T.; Fors, B. P. "Shaping" the Future of Molecular Weight Distributions in Anionic Polymerization. *ACS Macro Lett.* **2016**, *5*, 796–800.

(21) Gentekos, D. T.; Fors, B. P. Molecular Weight Distribution Shape as a Versatile Approach to Tailoring Block Copolymer Phase Behavior. *ACS Macro Lett.* **2018**, *7*, 677–682.

(22) Gentekos, D. T.; Jia, J.; Tirado, E. S.; Barteau, K. P.; Smilgies, D.-M.; DiStasio, R. A.; Fors, B. P. Exploiting Molecular Weight Distribution Shape to Tune Domain Spacing in Block Copolymer Thin Films. *J. Am. Chem. Soc.* **2018**, *140*, 4639–4648.

(23) Matyjaszewski, K.; Nakagawa, Y.; Gaynor, S. G. Synthesis of well-defined azido and amino end-functionalized polystyrene by atom transfer radical polymerization. *Macromol. Rapid Commun.* **1997**, *18*, 1057–1066.

(24) Mai, Y.; Eisenberg, A. Self-assembly of block copolymers. *Chem. Soc. Rev.* **2012**, *41*, 5969–5985.

(25) Hansen, C. M.; Andersen, B. H. The Affinities of Organic Solvents in Biological Systems. *Am. Ind. Hyg. Assoc.* **1988**, *49*, 301–308.

(26) Hansen, C. M. The Universality of the Solubility Parameter. *Ind. Eng. Chem. Prod. Res. Dev.* **1969**, *8*, 2–11.

(27) Ho, D. L.; Glinka, C. J. New insights into Hansen's solubility parameters. *J. Polym. Sci. B* **2004**, *42*, 4337–4343.

(28) Mieczkowski, R. The determination of the solubility parameter components of polystyrene by partial specific volume measurements. *Eur. Polym. J.* **1988**, *24*, 1185–1189.

(29) Sagalowicz, L.; Michel, M.; Adrian, M.; Frossard, P.; Rouvet, M.; Watzke, H. J.; Yaghmur, A.; De Campo, L.; Glatter, O.; Leser, M. E. Crystallography of dispersed liquid crystalline phases studied by cryo-transmission electron microscopy. *J. Microsc.* **2006**, *221*, 110–121.

(30) Hyde, S. T. Microstructure of bicontinuous surfactant aggregates. *J. Phys. Chem.* **1989**, *93*, 1458–1464.

(31) Templer, R. H.; Seddon, J. M.; Duesing, P. M.; Winter, R.; Erbes, J. Modeling the Phase Behavior of the Inverse Hexagonal and Inverse Bicontinuous Cubic Phases in 2:1 Fatty Acid/Phosphatidylcholine Mixtures. *J. Phys. Chem. B* **1998**, *102*, 7262–7271.

(32) Tyler, A. I. I.; Barriga, H. M. G.; Parsons, E. S.; McCarthy, N. L. C.; Ces, O.; Law, R. V.; Seddon, J. M.; Brooks, N. J. Electrostatic swelling of bicontinuous cubic lipid phases. *Soft Matter* **2015**, *11*, 3279–3286.

국문초록

분자량 분포가 없는 친수성 블록을 가진 블록 공중합체의 수용액 상 자기조립에 대한 소수성 블록의 분자량 분포의 영향

블록 공중합체를 이루는 고분자 블록의 분자량 분포는 벌크에서의 자기조립과 그 결과로 만들어지는 규칙적인 나노구조에 직접적으로 영향을 미친다고 알려져 있다. 하지만 블록 공중합체의 소수성 블록의 분자량 분포가 수용액 상 자기조립의 결과로 얻어지는 매우 규칙적인 메소 결정상에 미치는 영향에 대해서는 연구된 바가 드물다. 이 연구에서 우리는 소수성 블록의 분자량 분포가 수용액 상에서의 블록 공중합체의 복연속성 입방 메소 결정상에 미치는 영향에 대해서 논의하고자 한다. 구체적으로 말하자면, 분자량 분포가 없는, 즉 분산도가 1.0 인 폴리에틸렌글리콜 사슬을 갖는 친수성 블록과 원하는 분자량 분포를 갖는 소수성의 폴리스티렌 블록을 결합하여 다양한 소수성 블록의 분자량 분포를 갖는 일련의 블록 공중합체를 합성하였다. 이 때, 원자 전달 라디칼 중합 과정에서 개시제의 첨가 속도를 조절함으로써 폴리스티렌 블록의 분산도를 1.08 에서 1.72 까지 조절하였다.

이렇게 합성된 블록 공중합체의 수용액 상 자기조립의 결과로, 분산도가 증가할수록 폴리머 큐보좀의 내부 구조의 규칙성이 입방 결정상에서 불규칙한 구조를 갖는 스폰지 상으로 저하되는 것을 관찰하였다. 따라서, 내부 코어를 이루는 소수성 블록의 분자량 분포가 폴리머 큐보좀의 내부 구조의 규칙성을 결정하는 데에 있어서 주요한 변수로 작용한다는 것을 확인하였다. 또한, 폴리스티렌 블록의 수평균 분자량을 일정하게 유지한 채로 분산도를 올렸을 때, 관찰되는 폴리머 큐보좀의 대칭 구조가 $Pn\bar{3}m$ 에서 $Im\bar{3}m$ 이 우세해지는 것을 확인하였다.

주요어 : 블록 공중합체, 분자량 분포, 수용액 상 자기조립, 큐보좀

학 번 : 2017-24686